EC
Journals.ASM.org

The Response of *Nannochloropsis gaditana* to Nitrogen Starvation Includes *De Novo* Biosynthesis of Triacylglycerols, a Decrease of Chloroplast Galactolipids, and Reorganization of the Photosynthetic Apparatus

Diana Simionato,[a] Maryse A. Block,[b,c,d,e] Nicoletta La Rocca,[a] Juliette Jouhet,[b,c,d,e] Eric Maréchal,[b,c,d,e] Giovanni Finazzi,[b,c,d,e] Tomas Morosinotto[a]

Dipartimento di Biologia Università di Padova, Padua, Italy[a]; Laboratoire de Physiologie Cellulaire et Végétale, Unité Mixte Recherche 5168, Centre National Recherche Scientifique,[b] Université Grenoble 1,[c] Institut National Recherche Agronomique,[d] and Commissariat à l'Energie Atomique et Energies Alternatives, Institut de Recherches en Technologies et Sciences pour le Vivant,[e] Grenoble, France

Microalgae of the genus *Nannochloropsis* are capable of accumulating triacylglycerols (TAGs) when exposed to nutrient limitation (in particular, nitrogen [N]) and are therefore considered promising organisms for biodiesel production. Here, after nitrogen removal from the medium, *Nannochloropsis gaditana* cells showed extensive triacylglycerol accumulation (38% TAG on a dry weight basis). Triacylglycerols accumulated during N deprivation harbored signatures, indicating that they mainly stemmed from freshly synthesized fatty acids, with a small proportion originating from a recycling of membrane glycerolipids. The amount of chloroplast galactoglycerolipids, which are essential for the integrity of thylakoids, decreased, while their fatty acid composition appeared to be unaltered. In starved cells, galactolipids were kept at a level sufficient to maintain chloroplast integrity, as confirmed by electron microscopy. Consistently, N-starved *Nannochloropsis* cells contained less photosynthetic membranes but were still efficiently performing photosynthesis. N starvation led to a modification of the photosynthetic apparatus with a change in pigment composition and a decrease in the content of all the major electron flow complexes, including photosystem II, photosystem I, and the cytochrome b_6f complex. The photosystem II content was particularly affected, leading to the inhibition of linear electron flow from water to CO_2. Such a reduction, however, was partially compensated for by activation of alternative electron pathways, such as cyclic electron transport. Overall, these changes allowed cells to modify their energetic metabolism in order to maintain photosynthetic growth.

Microalgae are receiving increased attention as possible feedstock for biofuels production (1, 2). In particular, their reserves are considered a promising source of oil which can be converted into biodiesel by *trans*-esterification (3). The molecular structure of oil is a triacylglycerol (TAG), a glycerolipid made of a 3-carbon glycerol backbone esterified with three fatty acids. Glycerolipids in the biomass of photosynthetic cells consist of TAGs but also of membrane glycerolipids that are esterified with two fatty acids and that harbor a phosphorus-containing polar head (i.e., phospholipids) or a phosphorus-free polar head (e.g., glycolipids). Some microalgae and photosynthetic protists are able to accumulate large amounts of lipids (4–8). High lipid contents are achieved under nutrient limitation, with nitrogen (N) deprivation being particularly effective (6, 9–11). Nitrogen limitation affects photosynthesis by reducing the efficiency of light harvesting and of photochemical use of absorbed energy. This is due to a decrease in the chlorophyll (Chl) content as well as in the amount of photosynthetic complexes. This inhibition of photosynthesis ultimately hampers growth (12–15) in the accumulation of TAGs, while it fuels a reallocation of carbon fluxes. Laboratory studies have started unveiling information on the molecular mechanisms of photosynthesis inhibition under nutrient deprivation (16). For example, functional studies in green algae and diatoms have indicated a differential sensitivity of the photosynthetic complexes to nutrient starvation: while photosystem II (PSII) is particularly affected by N and sulfur (S) limitation (13), PSI seems to be more resistant to these starvations, while it is more sensitive to iron (Fe) deprivation (13, 17).

Species belonging to the *Nannochloropsis* genus are considered an emerging model to study algal biology, because of their high growth rate, the availability of tools for genetic manipulation (18, 19), and their ability to accumulate large amounts of oil (6, 8), which make them promising candidates for biodiesel production. The *Nannochloropsis* genus belongs to the Eustigmatophyceae and is mainly composed of species living in a coastal environment. They have cells of reduced size (~3 μm) and present a single chloroplast that is encircled by four membranes and that occupies most of the cell volume. They also have a peculiar pigment content, presenting only chlorophyll *a* and lacking other accessory chlorophylls, such as Chl *b* or *c*. Violaxanthin and vaucheraxanthin are the most represented carotenoids (Car) in the cells (20, 21). Although it has been documented that exposure of *Nannochloropsis* to N deprivation results in a large accumulation of oil (6), no clear picture of the changes occurring in their chloroplasts

Received 21 December 2012 Accepted 25 February 2013
Published ahead of print 1 March 2013
Address correspondence to Tomas Morosinotto, tomas.morosinotto@unipd.it, or Giovanni Finazzi, giovanni.finazzi@cea.fr.
Supplemental material for this article may be found at http://dx.doi.org/10.1128/EC.00363-12.

doi:10.1128/EC.00363-12

during this starvation has been provided so far. This information is fundamental because chloroplast activity provides the link between light photochemical conversion (which produces energy in the thylakoid membranes), carbon assimilation, and fatty acid biosynthesis (22, 23), which transforms this energy in the chloroplast stroma and envelope.

To provide a comprehensive picture of the changes occurring in the *Nannochloropsis* chloroplast during nitrogen starvation, we performed a detailed biochemical and physiological characterization of *Nannochloropsis gaditana* cells after exposure to N limitation. We showed that the sustained triacylglycerol accumulation triggered under these conditions is due to both *de novo* biosynthesis of fatty acids and recycling of membrane polar glycerolipids. Despite some degradation, membrane glycerolipids and, in particular, galactolipids are nevertheless kept to a level within the cell sufficient to avoid impairment of photosynthetic membrane integrity. We also observed a major reorganization of the photosynthesis chain, which comprises a decrease in the content of the major electron flow complexes (PSII, PSI, and the cytochrome [Cyt] b_6f complex) and an increase in the efficiency of alternative electron pathways, such as cyclic electron flow (CEF). Thanks to these responses, photosynthesis remains operational in *Nannochloropsis* cells even in the absence of an N supply to provide energy and reduce power for cell division and lipid biosynthesis.

MATERIALS AND METHODS

Culture conditions. *Nannochloropsis gaditana* strain 849/5 from CCAP was grown in sterile filtered F/2 medium (24), using sea salts (32 g/liter) from Sigma, 40 mM Tris HCl, pH 8, and the Sigma Guillard (F/2) marine water enrichment solution (containing $NaNO_3$ [0.075 g/liter]). Maintenance and propagation of cultures were performed using the same medium supplemented with 10 g/liter of plant agar (Duchefa Biochemie). Growth experiments were performed in Erlenmeyer flasks with orbital shaking, starting from a preculture grown at 100 μmol of photons m^{-2} s^{-1} at exponential phase. The preculture was diluted to an optical density at 750 nm (OD_{750}) equal to 0.4, corresponding to $\sim 1.7 \times 10^7$ cells/ml (final volume, 150 ml). Algal growth was maintained for 4.5 days (preinoculum), and then the cells were centrifuged at a relative centrifugal force of 2,500 (Allegra 250; Beckman) for 10 min at room temperature and resuspended in two different F/2 media, with one presenting nitrogen at the same concentration as that in the preculture and the other completely deprived of any nitrogen source. Both cultures were rediluted to an OD_{750} of 0.4. Growth was then performed for another 7 days. Illumination was constantly provided at 100 μmol of photons m^{-2} s^{-1}, using daylight fluorescent lamps. The temperature was kept at 23 ± 1°C in a growth chamber. Algal growth was measured spectrophotometrically by determination of the daily changes in the OD_{750} (Lambda Bio 40 UV-visible [UV-VIS] spectrometer; PerkinElmer), and cell number was monitored with a Bürker counting chamber (HBG, Germany) under a light microscope. All curves were repeated at least four times.

Glycerolipid analysis. Glycerolipids (i.e., membrane glycerolipids containing 2 fatty acids and triacylglycerols containing 3 fatty acids) were extracted from 10 mg of freeze-dried *Nannochloropsis gaditana* cells as described previously (25). Cells were frozen in liquid nitrogen immediately after harvest. The freeze-dried cell pellet was resuspended in 4 ml of boiling ethanol for 5 min, followed by the addition of 2 ml of methanol and 8 ml of chloroform at room temperature. The mixture was then saturated with argon and stirred for 1 h at room temperature. After filtration through glass wool, cell remains were rinsed with 3 ml of chloroform-methanol (2:1, vol/vol). In order to initiate biphase formation, 5 ml of 1% NaCl was then added to the filtrate. The chloroform phase was dried under argon before resolubilization of the lipid extract in pure chloroform. Overall, this method has the advantage that the use of boiling ethanol facilitates solvent penetration inside the cells and prevents lipid degradation during extraction. To isolate TAGs, lipids were run on silica gel plates (Merck) with hexane-diethyl ether-acetic acid (70:30:1, vol/vol). On the other hand, to isolate polar glycerolipids, lipids were analyzed on silica gel plates (Merck) by two-dimensional thin-layer chromatography (2D-TLC). The first solvent was chloroform-methanol-water (65:25:4, vol/vol), while the second one, after a 90° rotation, was chloroform-acetone-methanol-acetic acid-water (50:20:10:10:5, vol/vol). Lipids were then visualized under UV light after pulverization of 8-anilino-1-naphthalenesulfonic acid at 2% in methanol. They were then scraped off the 2D-TLC plates for further analyses. For mass spectrometric (MS) analysis, lipids were recovered by the method of Bligh and Dyer (26): the silica gel was resuspended in 1.35 ml chloroform-methanol (1:2, vol/vol) and mixed thoroughly before the addition of 0.45 ml chloroform and 0.8 ml H_2O. Lipids present in the chloroform phase were dried under argon and resuspended in 10 mM ammonium acetate in 100% methanol. They were introduced by direct infusion (electrospray ionization-MS/MS) into a mass spectrometer (LTQ-XL; Thermo Scientific) and identified by comparison with standards. Identification of each lipid class was performed by precursor or neutral loss analyses as described previously (27). For lipid quantification, fatty acids were methylated using 3 ml of 2.5% H_2SO_4 in methanol for 1 h at 100°C (including standard amounts of 21:0 fatty acids). The reaction was stopped by the addition of 3 ml of water and 3 ml of hexane. The hexane phase was analyzed by gas-liquid chromatography (PerkinElmer) on a BPX70 (SGE) column. Methylated fatty acids were identified by comparison of their retention times with those of standards and quantified by the surface peak method using 21:0 fatty acid for calibration. Extraction and quantification were done at least 3 times.

Electron microscopy. Pellets of different samples were fixed overnight at 4°C in 6% glutaraldehyde in 0.1 M sodium cacodylate buffer (pH 6.9) and postfixed for 2 h in 1% osmium tetroxide in the same buffer. The specimens were dehydrated in a graded series of ethyl alcohol and propylene oxide and embedded in araldite. Ultrathin sections (800 nm) cut with an ultramicrotome (Ultracut; Reichert-Jung, Vienna, Austria) and stained with lead citrate and uranyl acetate were then analyzed under a transmission electron microscope (Tecnai G2; FEI, Hillsboro, Oregon) operating at 100 kV.

Pigment extraction and analyses. Chlorophyll *a* and total carotenoids were extracted from *Nannochloropsis* centrifuged cells at 4°C with 100% *N*,*N*′-dimethylformamide (at least 50 μl/10^6 cells) for at least 48 h under dark conditions as described previously (28). Pigment concentrations were determined spectrophotometrically using specific extinction coefficients (29, 30).

High-pressure liquid chromatography (HPLC) analyses were carried out using a Beckman System Gold instrument equipped with a UV-VIS detector and a C_{18} column (25 cm by 4.6 mm; Zorbax octyldecyl silane). Pigments were extracted from cells frozen with liquid nitrogen using 80% acetone and mechanically broken in a mortar by addition of quartz sand. Runs were performed as described previously (31) using 86.7% acetonitrile, 9.6% methanol, and 3.6% Tris HCl, pH 7.8, as solvent A and 80% methanol and 20% hexane as solvent B. The peaks of each sample were identified through the retention time and absorption spectrum and quantified as described previously (31).

Western blot analyses of proteins from total cell extracts. The Cyt *f* and PsaA antibodies (raised against the *Chlamydomonas reinhardtii* proteins) were purchased from Agrisera (Sweden). The antibody against D2 was homemade using spinach protein. Gels were loaded with solubilized cell extracts corresponding to 52×10^6, 26×10^6, 13×10^6, or 6.5×10^6 cells, depending on the sensitivity of the specific antibody. The sample was solubilized in a buffer (3×) contained 30% glycerol, 125 mM Tris, pH 6.8, 0.1 M dithiothreitol, 9% SDS. SDS-PAGE analysis was performed with a Tris-glycine buffer system as described previously (32) with acrylamide at a final concentration of 12%. Western blot analyses were performed using nitrocellulose (Pall Corporation).

Spectroscopic analysis. Spectroscopic analysis was performed *in vivo* using a JST-10 spectrophotometer (Biologic, France). Changes in the amount of functional photosynthetic complexes were evaluated by measuring the electrochromic shift (ECS) spectral change, a shift in the pigment absorption bands that is linearly correlated to the number of light-induced charge separations within the reaction centers (33). To perform this analysis, we first assessed the *in vivo* spectrum of the ECS in *Nannochloropsis gaditana* cells in the 480- to 550-nm range upon continuous illumination of 1,000 μmol of photons m^{-2} s^{-1}, as discussed earlier (34). On the basis of this spectrum, the PSI and PSII content was estimated from changes in the amplitude of the fast phase of the ECS signal (at 527 nm and 507 nm, where the positive and negative peaks of the signal, respectively, are located) upon excitation with a saturating laser flash (520 nm, 5-ns duration). The PSII contribution was evaluated from the decrease in the amplitude of the signal in samples poisoned with 3-(3,4-dichlorophenyl)-1,1-dimethylurea (DCMU; 80 μM) and hydroxylamine (HA; 4 mM), which irreversibly block PSII charge separation. PSI was estimated as the fraction of the signal that was insensitive to these inhibitors (34). Cytochromes *f*, b_6, and P_{700} were quantified by evaluating the maximum change in absorption for samples incubated with dibromothymoquinone (DBMIB; 150 μM). This compound blocks plastoquinol oxidation by the cytochrome b_6f complex. Therefore, it promotes the full oxidation of both PSI and cytochrome redox cofactors in the light, as required to quantify their relative content. Cyts *f* and b_6 were evaluated as the difference between the absorption at 554 nm and 563 nm and the absorption at a baseline drawn between 546 and 573 nm, respectively (35). P_{700} was measured at 705 nm. Measurements of linear electron flow (LEF) and cyclic electron flow (CEF), as well as the level of reduction of other alternative electron sinks, were deduced by measuring PSI turnover at 705 nm in untreated, DCMU-poisoned (to block linear flow), and DCMU- and DBMIB-treated samples (to block both linear and cyclic flows). Cyclic electron flow was then evaluated as the residual rate of reduction of P_{700}-positive (P_{700}^+) cells that was observed in the presence of DCMU but that was abolished by DBMIB addition.

Fluorescence and oxygen measurements. Cryogenic fluorescence spectra were recorded at 77 K using a spectrophotometer (JBeamBio, France) equipped with a USB2000$^+$ charge-coupled-device (CCD) array (Ocean Optics). Samples were loaded into a small metal cuvette (volume, ~15 μl), which was directly immersed in the liquid nitrogen bath. Excitation was provided by a light-emitting diode source (peak at 450 nm; full width at half maximum [FWHM], ~20 nm), which was directed onto the sample through an optical guide. Emitted light was directed to the CCD array using a second fiber equipped with an RG 695 filter to remove the excitation light.

In vivo chlorophyll fluorescence was determined using a Dual PAM 100 system (Walz, Germany). After 20 min of dark adaptation, the parameter F_v/F_m was calculated as $(F_m - F_0)/F_m$, where F_v is the dark-adapted variable fluorescence, F_m is the maximum fluorescence, and F_0 is the dark-adapted fluorescence (36). Fluorescence kinetics was measured using a JTS10 spectrophotometer in the fluorescence mode. Fluorescence inductions were measured in the infrared region of the spectrum upon excitation with blue light at 450 nm. DCMU was added at a concentration of 80 μM to prevent oxidation of the primary quinone acceptor Q_A. In the presence of this inhibitor, an average of 1 photon per PSII center is absorbed at time *t* (37). This parameter was estimated for every fluorescence induction trace to evaluate the number of photons absorbed by photosystem II, i.e., the antenna size. Oxygen evolution under saturating light (1500 μE m^{-2} s^{-1}) was measured using a Clark electrode (Hansatech, United Kingdom) as described previously (38), and rates were calculated when cells reached a steady state.

RESULTS

Effects of nitrogen availability on *Nannochloropsis* growth and lipid content. *Nannochloropsis gaditana* was grown in batch cultures in continuous light at an intensity of 100 μmol of photons m^{-2} s^{-1}. In order to ensure the standardization of the preinoculum, cells were first grown for 4.5 days in an F/2 medium containing nitrogen (0.075 g/liter $NaNO_3$). Cells were then harvested and used to inoculate two cultures, one with the same fresh medium with nitrogen (N^+) and another with a medium completely lacking nitrogen (N^-). Cultures were grown under these conditions for another 7 days. Growth kinetics, reported in Fig. 1A, show that *Nannochloropsis* maintained the ability to growth under N^- conditions at least for a few days, although with a reduced rate with respect to that for cells grown under N^+ conditions (N^+ cells). This was confirmed by measurements of the dry weight, which after 5 days was similar in N^+ cells and cells grown under N^- conditions (N^- cells) (0.43 ± 0.03 and 0.46 ± 0.05 g/liter, respectively). Treatment of N^- cells with DCMU, a specific inhibitor of photosystem II, completely blocked growth (Fig. 1A), suggesting that in nitrogen-starved cultures, cell duplication was completely dependent on photosynthetic activity and did not rely on consumption of energy reserves (e.g., carbohydrates).

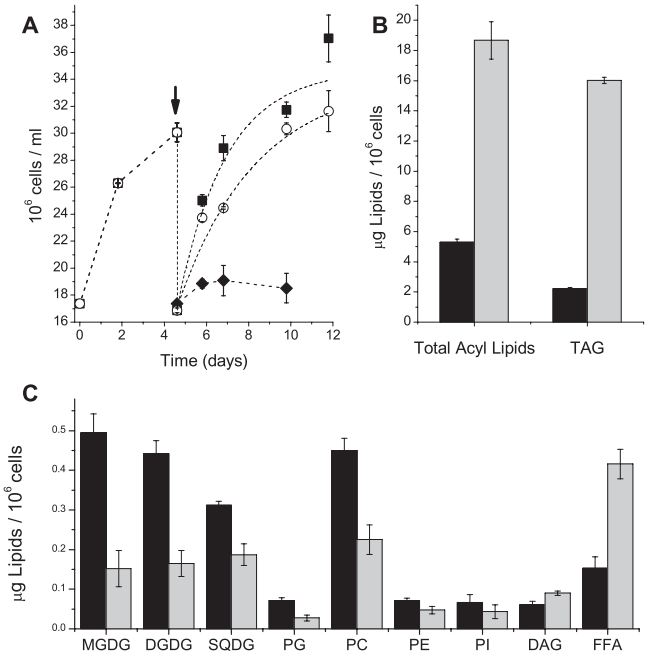

FIG 1 Growth and lipid accumulation in *Nannochloropsis gaditana* cultures with nitrogen excess or nitrogen deprivation. (A) Cells were grown for 4.5 days in a nitrogen-rich medium and then harvested and split into two other media (as indicated by the arrow): one N rich (black squares) and the other completely lacking of any additional N source (empty circles). Cells grew for another 7 days under these conditions. Black diamonds, nitrogen-starved cells treated with 1 μM DCMU. Data are averages of at least four independent replicates. (B and C) Lipid quantification in *Nannochloropsis* cells. (C) Results for the major lipid classes, MGDG, DGDG, SQDG, phosphatidylglycerol (PG), PC, phosphatidylethanolamine (PE), phosphatidylinositol (PI), DAGs, and FFAs, isolated from *Nannochloropsis gaditana* cultures. Black bars, nitrogen-replete conditions; gray bars, nitrogen-starved conditions.

As shown in Fig. 1B, nitrogen depletion induced a strong increase in the total fatty acid (i.e., acyl lipid) content of cells, which is correlated with a strong accumulation of TAGs. Reciprocally, the content in polar glycerolipids, mostly represented by monogalactosyl-diacylglycerol (MGDG), digalactosyl-diacylglycerol (DGDG), sulfoquinovosyl-diacylglycerol (SQDG), and phosphatidylcholine (PC), is reduced by a factor of ~1.5 to 3, depend-

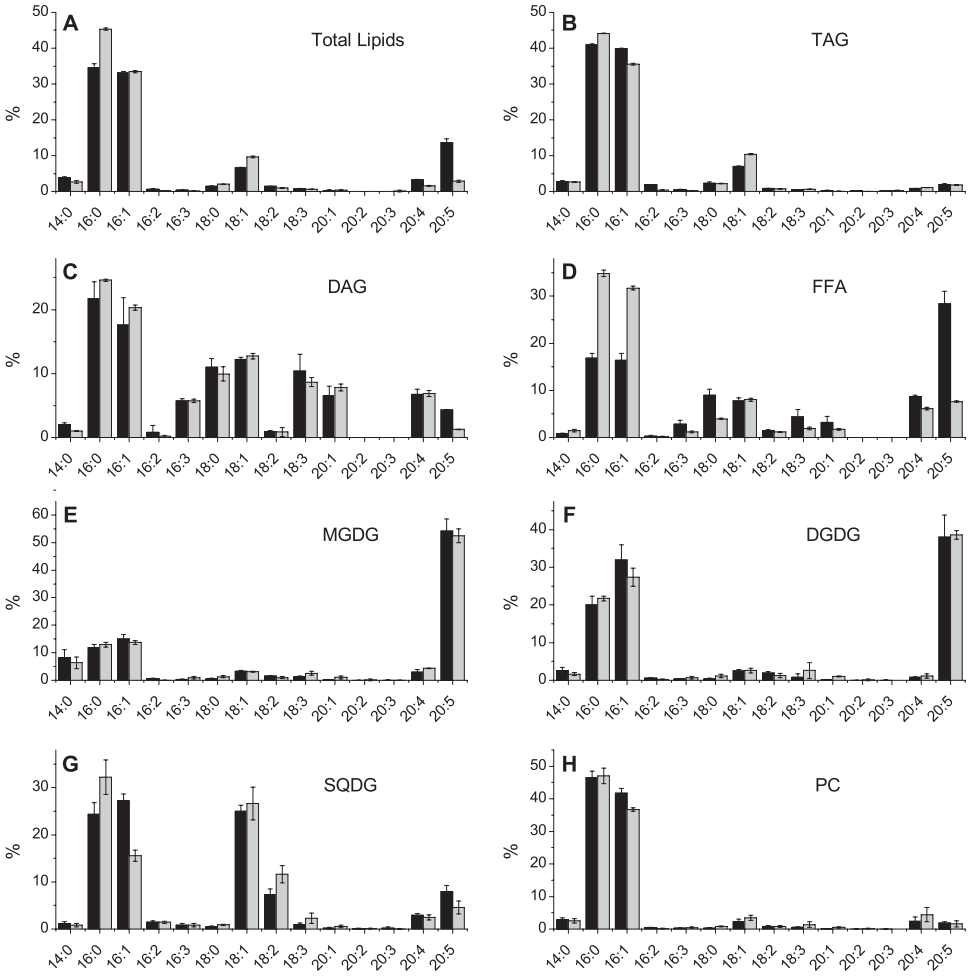

FIG 2 Fatty acid profiles of *Nannochloropsis gaditana* major lipid classes. Results are shown for total lipid extracts (A) and some of the major lipid classes, TAGs (B), DAGs (C), FFAs (D), MGDG (E), DGDG, (F), SQDG (G), and PC (H), isolated from *Nannochloropsis gaditana* cultures grown under nitrogen-replete (black bars) or nitrogen-starved (gray bars) conditions. Several lipid classes change in fatty acid composition, while some others look more stable. In total lipids, nitrogen starvation induces a marked increase in 16:0 fatty acid proportions and a decrease in 20:5 fatty acid proportions, whereas the TAG modification of the fatty acid profile is rather low. We observe in TAGs a slight increase in 16:0 and 18:1 fatty acid proportions and a slight decrease in 16:1 fatty acid proportions. The 20:4 and 20:5 fatty acid proportions in TAGs remain stable and low. The FFA composition is deeply modified, with a sharp increase in 16:0 and 16:1 fatty acids and a sharp decrease in 20:5 fatty acids occurring. In contrast, the MGDG and DGDG fatty acid composition and, to a lower extent, the DAG fatty acid composition remain stable.

ing on the lipid class (Fig. 1B and C). MGDG is the most affected lipid, with a reduction of about two-thirds. Free fatty acid (FFA) content, which was initially in the same range as that of the individual polar glycerolipids, almost doubled in N^- cells, suggesting a higher release of fatty acids in this sample (Fig. 1C). Taking into account the changes in the lipid content per cell (Fig. 1), as well as the number of cells per gram of dry weight, we calculated that the absolute increase in TAGs (70 to 380 μg/mg of dry weight, thus reaching 38% of the total biomass) is much larger than the decrease in polar glycerolipids (from 60 to 20 μg/mg dry weight, i.e., about 10 to 15% of the overall TAG increase; Fig. 1; see Materials and Methods). This finding excludes the possibility that TAGs exclusively originated from the recycling of preexisting membrane glycerolipids. Instead, this finding suggests that substantial *de novo* synthesis of fatty acid chains occurred in N^- cells following an active glycerolipid biosynthesis. This conclusion is also supported by the finding that the diacylglycerol (DAG) content is increased in N^- cells (Fig. 1C).

In general, TAGs can be produced by two main routes in a cell: (i) *de novo* synthesis of fresh fatty acids directly incorporated into TAGs via the Kennedy pathway or (ii) conversion of preexisting polar glycerolipids (27). TAGs generated by the first route contain fatty acids harboring the molecular signature of fresh synthesis, i.e., high levels of 16:0 and 18:1 fatty acids. On the other hand, TAGs obtained from recycling of membrane glycerolipids contain fatty acids with the molecular signature of their original lipid classes, i.e., with a substantial proportion of elongated and polyunsaturated molecular species such as 20:5 fatty acids (39, 40). In order to get further insights into the possible origins of the TAGs formed in N^- cells, we performed a detailed analysis of the fatty acid composition of *N. gaditana* lipids, including polar glycerolipids, TAGs, FFAs, and DAGs (Fig. 2), focusing on the 20:5 fatty acid content of each lipid class. This content of 20:5 fatty acids allows estimation of the extent of polar lipid conversion into TAGs during nitrogen deprivation (Fig. 3). Clearly, N starvation results in a decrease of the 20:5 fatty acid level in total lipids, which results

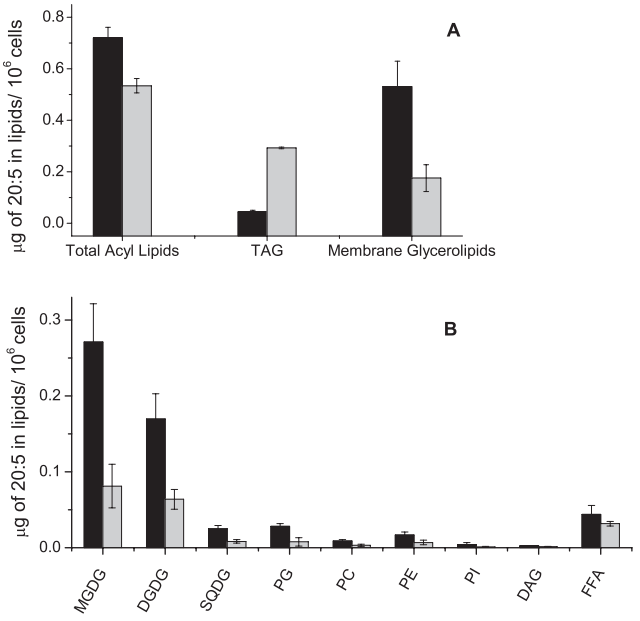

FIG 3 Quantification of 20:5 fatty acids in the major lipid species per 10^6 *Nannochloropsis gaditana* cells grown with nitrogen excess or nitrogen deprivation. *Nannochloropsis* cells were grown under nitrogen-replete and -starved conditions (black and gray bars, respectively). (A) Quantification in total lipid extracts, TAGs, and total membrane glycerolipids; (B) quantification of major lipid classes, MGDG, DGDG, SQDG, phosphatidylglycerol (PG), PC, phosphatidylethanolamine (PE), phosphatidylinositol (PI), DAGs, and FFAs.

from both TAG neosynthesis and a polar lipid decrease. Most of the decrease of the 20:5 fatty acid level in polar lipids is correlated with the decline of MGDG and DGDG, which suggests that a conversion of galactolipids into TAGs has occurred during nitrogen starvation, even if it does not represent the main source of TAG production.

Since galactolipids are typically found in the thylakoid membranes, this finding additionally indicates that the content of photosynthetic membranes is reduced under conditions of nitrogen starvation. On the other hand, the fatty acid composition of the remaining galactolipids is not significantly changed between N^+ and N^- conditions (Fig. 2). Since these lipids are the main components of the thylakoid membranes, this suggests that the integrity of chloroplast membranes is likely maintained in *Nannochloropsis* N^- cells.

Influence of nitrogen availability on cell structure. In order to verify this hypothesis, we compared the chloroplast structures in cells growing for 5 days in N^+ or N^- medium using transmission electron microscopy. This time point was chosen for all following analyses presented because it allows observation of the N-depletion responses before the onset of a stress that is too severe. As shown in Fig. 4A to D, different organelles are well visible in N^+ cells and the chloroplast occupies a significant part of the cell volume. Thylakoids are organized as stacks of three membranes, a structure which is typical of this species. It is also worth underlining that small oil bodies, which are typically less electron opaque than other cellular structures, such as the protein-rich thylakoid membranes, are visible in some N^+ cells, and examples of these cases are shown in Fig. 4C and D. This suggests that these cells may also be subjected to some nutrient stress, although to a minor extent compared to that for N^- cells, where a major fraction of the cell volume was occupied by oil bodies (Fig. 4E to H). Depending on the specific region where the section was cut, some N^- cells appear to be completely occupied by oil bodies (Fig. 4H). However, even under nitrogen deprivation, cellular organelles are still well identifiable. Chloroplasts also appear intact, and the thylakoid membrane organization is very similar to the one observed in N^+ cells.

Effects of nitrogen excess or deprivation on *Nannochloropsis* photosynthetic activity. To test the possible consequences of N starvation on photosynthesis, we measured changes in the photo-

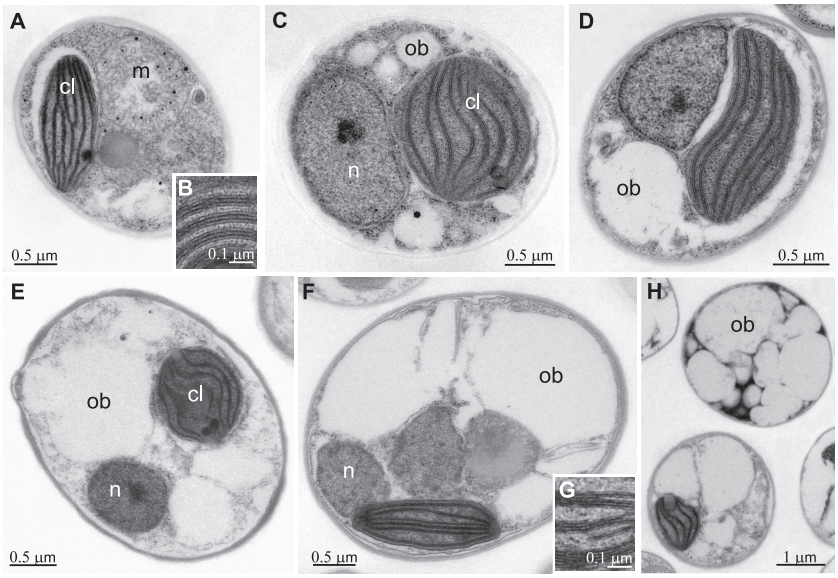

FIG 4 Transmission electron microscopy of N-replete and N-starved *Nannochloropsis* cells. (A to D) N^+ cells; (E to H) examples of N^- cells. Panels B and G show enlargements focusing on the thylakoid membrane organization in N^+ and N^- cells, respectively. Organelles are indicated as follows: n, nucleus; m, mitochondria; cl, chloroplast; ob, putative oil bodies.

TABLE 1 Pigment composition of *Nannochloropsis* cells grown with different nitrogen availabilities[a]

Growth condition	Chl content (μg Chl *a*/10^6 cells)	Chl/Car ratio
N^+	0.15 ± 0.02	2.86 ± 0.05
N^-	0.07 ± 0.03	2.54 ± 0.08

[a] *Nannochloropsis* cultures were grown for 5 days under N^+ and N^- conditions.

synthetic apparatus after 5 days of N depletion. We first observed a strong decrease (about 50%; Table 1) in Chl content per cell in the N^- culture compared to that in the N^+ culture. This is consistent with the findings of galactolipid analyses, supporting the concept that the amount of photosynthetic membranes should be reduced in these cells. The observed decrease in the Chl/Car ratio in N^- cells from ~2.9 to ~2.6 (Table 1) also suggests a relative increase in the carotenoid content, as is often observed in case of stress. Consistent with this possibility, HPLC analysis of N^- cells revealed relative increases in violaxanthin, anteraxanthin, and zeaxanthin, the carotenoids participating in the xanthophyll cycle (41), while their precursor, β-carotene, was diminished (Table 2). The content of the secondary carotenoid cantaxanthin was also significantly enhanced in N^- cells.

Possible changes in the overall photosynthetic capacity during nitrogen starvation were investigated using the F_v/F_m parameter, which provides an estimate of the photosystem II quantum yield (42, 43). While N^+ cells maintained a high F_v/F_m for the whole growth period analyzed, N-starved cells showed instead a progressive decrease in this parameter to 0.49, down from 0.60 (Fig. 5A), indicating a progressive reduction of their PSII activity. Photosystems are composed of two moieties: a core complex responsible for the photochemical reactions and an antenna system which is involved in light harvesting. Therefore, changes in F_v/F_m [i.e., in the $(F_m - F_0)/F_m$ ratio] could stem either from a direct modification of the reaction center amount/activity (which can increase the F_0 parameter or decrease the F_m parameter) or from an energetic uncoupling of the antenna from the reaction center. The latter phenomenon also leads to the increase in the fluorescence yield at F_0 and, therefore, to a decrease in the F_v parameter. To verify if the reduction of the PSII efficiency measured in N^- cells was due to changes in the reaction center activity or to a modification of the energy transfer between the antennae and the core, we first measured the fluorescence spectra at cryogenic temperatures. Figure 5B confirms the reduced PSII content in N^- cells compared with that in N^+ cells, as indicated by the diminished ratio between the PSII emission peaks (685 and 695 nm) and the PSI emission peak (735 nm). However, no evidence for the presence of weakly coupled light-harvesting proteins in either cell type was found, as shown by the absence of an emission shoulder below 680 nm, a region where emission from uncoupled antenna is expected (44). Thus, these spectra demonstrate that the antenna complexes are capable of efficiently transferring energy to reaction

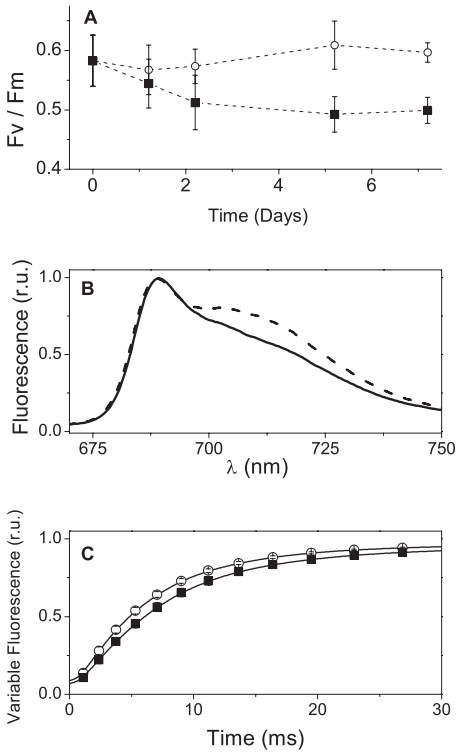

FIG 5 Photosystem II photochemical activity and photosynthesis efficiency in *Nannochloropsis* cells during nitrogen starvation. (A) Photosystem II efficiency was monitored by determination of the F_v/F_m parameter during growth under N-replete (solid squares) and N-starved (open circles) conditions; (B) fluorescence of N^+ cells (solid line) and N^- cells (dashed) at 77 K; (C) fluorescence induction curve in dark-adapted cells treated with 10^{-6} M DCMU. Black squares and white circles, N^+ and N^- cells, respectively. r.u., relative units.

centers even in N^- cells. This conclusion was further substantiated by the finding that the rise of fluorescence in DCMU-poisoned cells was ~30% faster in N^- cells (upon normalization of the variable fluorescence; Fig. 5C). Because only a single charge separation can take place under these conditions, this rise is directly proportional to the optical section of the PSII reaction. Thus, the finding that absorption is larger in N^- cells than in N^+ cells confirms that all the antennae present in N^- cells are energetically coupled to the reaction center. Moreover, the observation of a larger amount of light-harvesting complexes bound to the PSII cores in nitrogen-starved cells is consistent with a significant reduction in the amount of PSII reaction centers (leading to an increase in the ratio of the antenna to PSII in N^- cells), in agreement with the decreased F_v/F_m ratio. Overall, we conclude that the PSII amount and/or activity is diminished under conditions of N starvation, in agreement with previous findings in other algae (13).

TABLE 2 Carotenoid composition of *N. gaditana* cells 5 days after resuspension under N-excess or N-deprived conditions

	No. of mol of carotenoid/100 mol Chl *a*[a]					
Nitrogen condition	Violaxanthin	Vaucheraxanthin	Anteraxanhin	Zeaxanthin	Cantaxanthin	β-Carotene
N^+	36.7 ± 1.3	15.6 ± 0.7	4.2 ± 0.3	3.2 ± 0.3	1.0 ± 0.1	7.6 ± 0.1
N^-	50.8 ± 4.3	18.0 ± 0.8	9.2 ± 1.2	9.2 ± 0.9	3.2 ± 1.0	4.6 ± 0.1

[a] Calculated from HPLC analysis.

Nitrogen depletion induces a large reorganization of the photosynthetic apparatus and activity in *Nannochloropsis*. The data reported above indicate that *Nannochloropsis* cells were able to support significant fatty acid biosynthesis under conditions of nitrogen deprivation, despite the decrease of thylakoid galactolipids and alterations in their photosynthetic activity. To further investigate this point, we measured possible changes in the composition/architecture of the photosynthetic complexes. First of all, we determined the PSII/PSI stoichiometry using the electrochromic shift (ECS). ECS is a change in the absorption spectrum of pigments embedded in the thylakoid membranes, which is generated by the building of an electric field ($\Delta\Psi$) across them. The field is produced by charge separation within the reaction centers of the two photosystems and by electron flow in the cytochrome b_6f complex and modifies the spectrum of pigment-containing complexes due to the Stark effect (33). When illuminated, *Nannochloropsis* cells displayed an ECS signal having spectral features similar to the one measured in green algae (Fig. 6A). However, the spectrum was significantly red shifted compared to a typical ECS spectrum measured in chlorophytes. This could reflect either the different nature of the carotenoids present in the light-harvesting complexes (20, 21) (Table 2) or a different protein environment experienced by these chromophores, as previously suggested (21). The ECS signal in *Nannochloropsis* cells was unchanged under nitrogen-replete and -starved conditions (Fig. 6A), indicating that despite the changes in the pigment composition, N deprivation did not affect the response of carotenoids to the electric field present across the thylakoid membranes.

When generated by a single-turnover saturating flash (a pulsed laser flash in our case), the ECS signal depends only on the amount of the photosynthetic complexes which perform charge separation. Its occurrence is not affected either by the light-harvesting capacity of the centers or by the efficiency of the soluble carriers, which both ensure electron flow between the two photosystems (34). Moreover, this signal has a linear response to the light-generated $\Delta\Psi$, and the amplitude of the fast ECS is proportional to the photochemical activity of both PSI and PSII. This allows evaluation of the relative amounts of the two photosystems, on the basis of their different sensitivities to the addition of the PSII inhibitors DCMU and HA (34) (Fig. 6B). Shortly, we attribute the fraction of the fast ECS that is insensitive to DCMU and HA to PSI photochemistry, while the signal abolished by the addition of the two inhibitors reflects PSII photochemistry. We observed a significant decrease in the PSII/PSI ratio in the N-depleted cells, which dropped from ~1 (in N^+ cells) to ~0.6 (in N^- cells) (Fig. 6C). In principle, the observed change in the PSII/PSI ratio could stem from either a decrease in PSII or an increase in the latter complex. To distinguish between these two possibilities, we evaluated the absolute amount of photosystem I in N^+ and N^- cells by measuring the maximum amount of photo-oxidable P_{700} (the primary electron donor to PSI) in the presence of DBMIB, a specific inhibitor of the cytochrome b_6f complex which prevents its rereduction by plastoquinol (34, 45). We found that the PSI content was reduced by a factor of ~2 in N-deprived cells (Fig. 7A and D) on a cell basis. Similar results (Fig. 7B to D) were obtained in the case of the cytochrome b_6f complex, which was quantified from the maximum amplitude of the absorption signals reflecting redox changes of cytochromes b_6 (563 nm; Fig. 7B and D) and f (554 nm; Fig. 7C and D) in DBMIB-treated samples. This indicates that all the major complexes involved in photosynthetic electron flow, including PSII and PSI and the cytochrome b_6f complex, are decreased upon N starvation, although PSII is the complex most sensitive to this treatment.

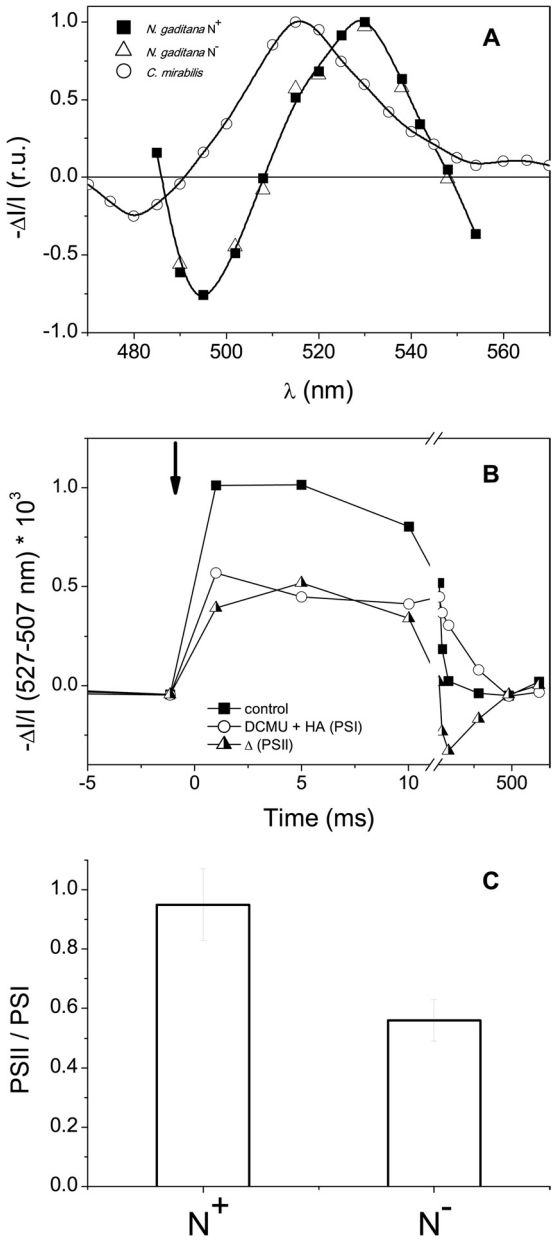

FIG 6 PSII/PSI ratio in *Nannochloropsis* cells. (A) Spectrum of the ECS signal in *Nannochloropsis gaditana* cells illuminated with continuous saturating light (1,000 μmol photons m^{-2} s^{-1}). The ECS signal is presented as the light minus dark absorption. Black squares and empty triangles, N^+ and N^- cells, respectively; white circles, the ECS spectrum measured in *Chlorella mirabilis* (34), reported for comparison. ΔI/I, (I [measuring cuvette] − I [reference cuvette])/I (reference cuvette), where I is the light intensity. (B) ECS kinetics of *Nannochloropsis* N^+ cells at 527 to 507 nm. Solid squares, kinetics under control conditions (N^+) reported as the total ECS signal; empty circles, measurement in the presence of DCMU and HA, where only PSI contributes to ECS; triangles, the difference in the signal attributable to PSII; arrow, the time when the single-turnover saturating flash was fired. (C) Quantification of the PSII/PSI ratio from the ECS signal at 527 nm minus the ECS signal at 507 nm in N^+ and N^- cells. See Materials and Methods for more details.

To confirm conclusions inferred from the spectroscopic anal-

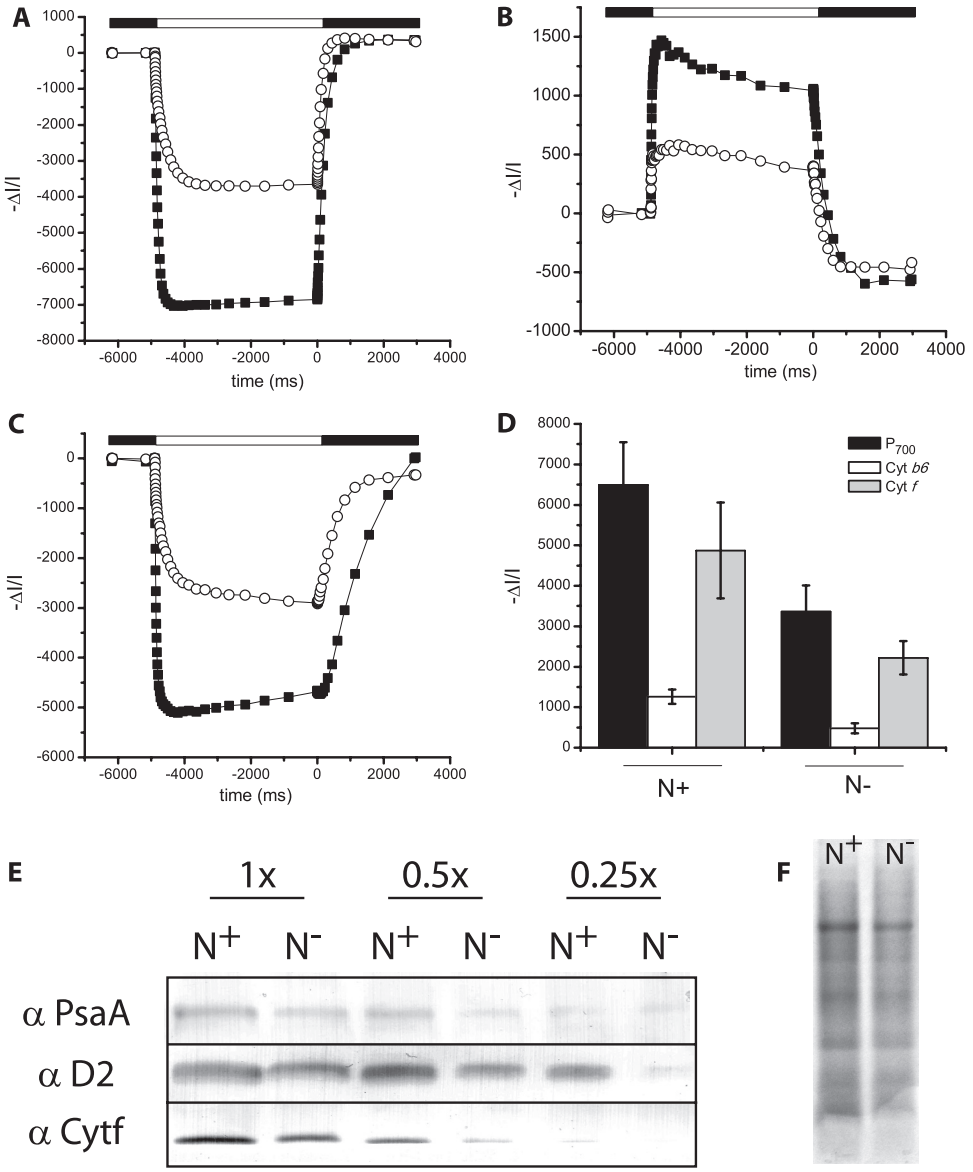

FIG 7 Quantification of the PSII, cytochrome b_6f, and PSI complexes in *Nannochloropsis* cells. Data refer to the same cell number (75×10^6 cells/ml). The PSI content was evaluated from the maximum absorption of P_{700}^+ at 705 nm (A), while the cytochrome b_6f complex was evaluated from signals related to Cyt b_6 at 563 nm (B) and Cyt *f* at 554 nm (C). Black squares, N^+ cells; empty circles, N^- cells; white box, actinic light on; black box, actinic light off. (D) Average values for P_{700}, Cyt b_6, and Cyt *f* in N^+ and N^- cells are shown. Data (± standard deviation) refer to 3 experimental replicates from 4 biological replicates. (E) Quantification of PSII, PSI, and Cyt *f* using specific antibodies. Protein extracts corresponding to the same number of cells (with 1× corresponding to 52×10^6 cells in the case of PsaA and Cyt *f* and 26×10^6 cells for D2) were loaded. In the case of D2, the antibody signal reached saturation in N^+ cells, as shown by the little difference between the 1× and 0.5× samples. (F) Coomassie-stained gel loading 13.5×10^6 cells.

ysis and verify the possible accumulation of inactive proteins in the membranes, we assessed the contents of the different photosynthetic complexes in N^+ and N^- cells using Western blotting analysis. To this aim, we exploited antibodies raised against proteins of the photosynthetic apparatus of other species which were able to recognize *Nannochloropsis* polypeptides with sufficient affinity. Figure 7E shows a clear decrease in the content of D2, PsaA, and Cyt *f* in N^- cells, which indicates a reduction in PSII, PSI, and Cyt b_6f complexes and thus confirms the results from the spectroscopic analysis and excludes a major accumulation of inactive polypeptides in the membranes.

The analysis presented above allows the conclusion that N deprivation has a deep impact on the composition of the photosynthetic apparatus in *Nannochloropsis*, with a general decrease of all complexes of the photosynthetic chain. The diminished concentration of photosynthetic complexes was also paralleled by a decrease in the rate of P_{700}^+ rereduction after illumination with continuous light (Fig. 8). This decrease, however, was not dramatic, since the electron transport rates went from 51.2 ± 7.2 electrons s^{-1} PSI^{-1} in N^+ cells to 36.4 ± 4.6 in N^- cells (Fig. 8C). This scenario was confirmed by the evaluation of the steady-state oxygen evolution capacity of N^+ and N^- cells, which showed a 28% reduction (Fig. 8E). Measurements of P_{700}^+ rereduction in the presence of the PSII inhibitor DCMU also indicate that cyclic

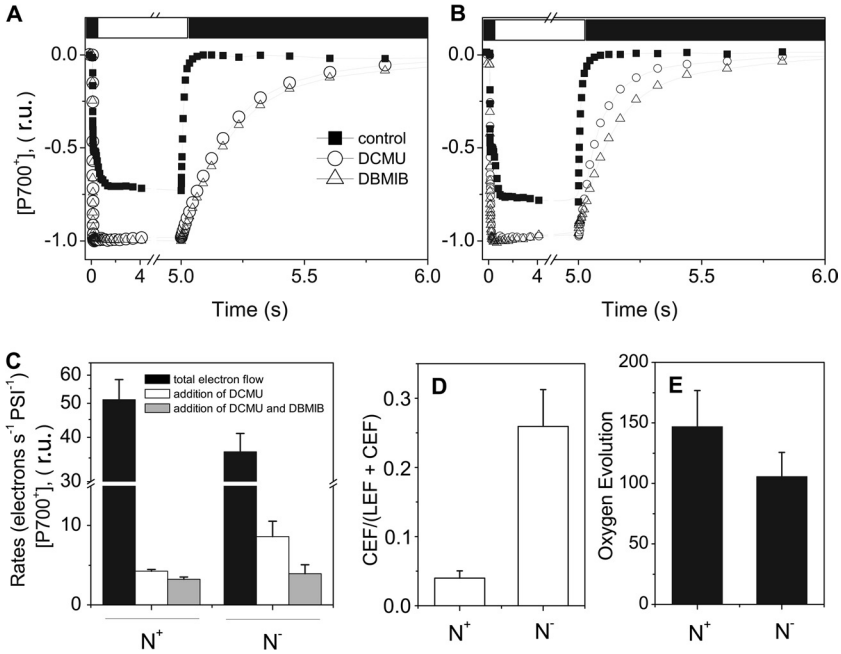

FIG 8 Spectroscopic quantification of the total and alternative electron flows under N excess and N deprivation conditions in *Nannochloropsis* cells. (A and B) P_{700} redox kinetics in N^+ and N^- cells, respectively, for control cells (solid squares) and cells treated with DCMU (open circles) and DCMU and DMIB (triangles). (C) Quantification of P_{700}^+ rereduction rates after illumination. Data refer to the rates measured in control, DCMU-treated, and DCMU- plus DBMIB-treated samples. Black column, total electron flow; white column, contribution of cyclic and other alternative electron flows after the addition of DCMU; gray column, other alternative electron flows after the addition of DCMU and DBMIB, which block linear and cyclic electron flows, respectively. Therefore, the black column minus the white column represents the linear electron flow, while the white column minus the gray column represents the cyclic electron flow. These calculations are reported in panel D. (E) Steady-state photosynthetic oxygen evolution (expressed as μmol O_2 mg Chl^{-1} h^{-1}) measured with a Clark electrode at saturating light intensity (1,500 μmol photons m^{-2} s^{-1}) ($n = 6$).

electron flow was not sensitive to nitrogen starvation. On the contrary, its efficiency was increased in N^- cells (Fig. 8D). Conversely, almost identical P_{700}^+ rereduction rates were measured in N^- and N^+ cells poisoned with DCMU and DBMIB (to block both LEF and CEF), ruling out the possibility that N starvation had opened the way to a specific alternative pathway to rereduce P_{700}^+. We therefore conclude that the major responses of the photosynthetic machinery to N starvation in *N. gaditana* were a reduction of PSII activity and therefore of linear electron flow, which was partially compensated for by an increased CEF turnover (Fig. 8D).

DISCUSSION

Growth and glycerolipid (membrane lipid and triacylglycerol) metabolism in nitrogen-starved *Nannochloropsis* cells. In this work, we addressed the response of *Nannochloropsis gaditana* to N starvation, i.e., the metabolic condition which is generally employed to induce lipid accumulation in the cells for biotechnological exploitation of this organism.

We first observed that *Nannochloropsis* cells were able to grow for 5 days under the N^- experimental conditions employed in this work. These conditions were chosen because they are representative of the conditions experienced by *Nannochloropsis* in its natural environment, although growth can largely be increased by providing excess nutrients and CO_2 (46). It is possible, however, that the influence of the nitrogen supply on growth rates is different under other conditions. Despite the lack of strong growth inhibition, N deprivation has a big impact on algal metabolism under the conditions tested in this work. We first found that although TAGs were detectable in N^+ cells (6), their concentrations were strongly increased under conditions of nitrogen deprivation, consistent with earlier findings (5). Moreover, the membrane glycerolipids decreased in N-starved cells. In principle, this may suggest that TAGs are produced at the expense of preexisting membrane lipids, which would be degraded during nitrogen starvation. Consistent with this hypothesis, we found that the levels of MGDG and DGDG, i.e., the most represented lipids of the thylakoid membranes, were reduced upon N starvation compared to their levels in N-replete cells. A survey of the content of the 20:5 fatty acid molecular species of the different lipid classes is also consistent with the occurrence of some recycling of 20:5 fatty acids from galactolipids to TAGs. These data support the existence of a galactolipid-to-TAG route similar to that recently described in *Chlamydomonas reinhardtii* (47). On the other hand, fatty acid recycling by membrane degradation is not sufficient to account for the large increase in TAGs. As already discussed above, the TAG content rose from 70 to 380 μg/mg of dry weight, while the polar glycerolipid content diminished from 60 to 20 μg/mg of dry weight (i.e., about 10 to 15% of the overall TAG increase; Fig. 1). Therefore, the massive accumulation of TAGs following nitrogen starvation cannot be accounted for only by lipid degradation; significant *de novo* fatty acid synthesis must also take place, combined with a small portion of polar lipid recycling.

Both growth and *de novo* fatty acid biosynthesis require a strong energy input, which could come from photosynthesis but which could also come from degradation of carbohydrate reserves accumulated under the N^+ conditions. The latter hypothesis, however, is not consistent with the observation that inhibition of

photosynthesis with DCMU not only prevents growth (Fig. 1A) but also reduces TAG accumulation down to 10% of the levels measured in N^+ cells. It therefore seems that in N^- cells both biomass and lipids are generated using energy derived from photosynthesis.

Modifications in the architecture of the photosynthetic apparatus of *Nannochloropsis* during nitrogen starvation. The observation that N-starved cells rely on photosynthesis to support growth and fatty acid biosynthesis led us to analyze in detail the features of the photosynthetic apparatus in N^- cells. Overall, N deprivation has a big impact on the chloroplast, which showed a reduced Chl content (Table 1). Carotenoids are also decreased, although to a lesser extent than chlorophyll, leading to an increased Car/Chl ratio, as is often observed in photosynthetic organisms under stress conditions (48). Exposure to light stress in N^- cells is also supported by the observation that carotenoids involved in the xanthophyll cycle (violaxanthin, anteraxanthin, and zeaxanthin) and the secondary carotenoid canthaxanthin are accumulated under this condition (Table 2), consistent with their role in protection from oxidative stress (20, 41).

Along with the decrease in pigment and in photosynthetic lipid content, the concentration of all the major complexes involved in photosynthetic electron flow was reduced in N^- cells, confirming that N starvation induces a global depression of the photosynthetic machinery in N^- *Nannochloropsis* cells. PSII is the main target of N limitation in *N. gaditana*, as shown by the decrease in the PSII/PSI ratio from ~1 to ~0.6 in N^- cells (Fig. 6). Such a decrease can be explained on the basis of the notion that the D1 subunit of this complex has a fast turnover in the light. Since this process relies on efficient protein biosynthesis (and therefore on N availability), it is tempting to propose that the overall D1 turnover may be affected by nitrogen depletion, leading to a higher light susceptibility of PSII and a consequent sustained degradation of this complex (49). The PSII centers left in N^- cells are, however, photochemically active, as revealed by their capacity to perform charge separation (Fig. 5A) and to evolve oxygen (Fig. 8E). They are also characterized by a larger antenna size, suggesting that the light-harvesting complexes are less affected than the reaction center itself under nitrogen starvation conditions and that they bind to the PSII core in a larger stoichiometry than in N^+ cells (Fig. 5B and C). The observation that the decreased PSII content has no major effects on biomass growth suggests that PSII photochemistry is not limiting photosynthesis under the conditions explored in this work. Other processes, e.g., CO_2 assimilation in the Calvin cycle or cytochrome b_6f complex turnover, which is the slowest step of electron flow in the thylakoids, are likely limiting growth under these conditions.

We indeed observed a decrease in the cytochrome b_6f amount upon N starvation (Fig. 7), as already reported in *Chlamydomonas reinhardtii*. However, in this green alga, the degradation of the complex is almost complete and seems to play a specific role in the activation of gametogenesis (50), a phenomenon which has not been observed so far in *Nannochloropsis*. On the other hand, the observed decrease in the content of PSI (~50%; Fig. 7) in N-starved cells has not been reported so far in other microalgae. Previous studies in the diatom *Thalassiosira weissflogii* and the chlorophyte *Dunaliella tertiolecta* have pointed out a relative stability of this complex in N-starved cells (13). This decrease could simply follow the degradation of the photosynthetic membranes, as suggested by the decrease in MGDG and DGDG, or represent a specific strategy of *Nannochloropsis* to mobilize more N for housekeeping purposes.

Nitrogen deprivation leads to changes in photosynthetic activity in *Nannochloropsis* by modifying the nature of the electron sink for light-generated PSI electrons. In N^- cells, we observed a clear but not drastic decrease in electron transport and oxygen evolution, suggesting that the residual complexes are still capable of driving electron flow to CO_2. Previous work in photosynthetic microorganisms (cyanobacteria, microalgae) has shown that ATP generation by LEF is generally the limiting factor for carbon assimilation in the light (51, 52). Therefore, the ATP required to feed other cellular processes (synthesis of proteins, DNA, lipids, etc.) which are essential to complete the cellular growth cycle is mostly produced by alternative electron flow pathways which generate ATP without producing NADPH (cyclic electron flow, the Mehler reaction) or by the respiratory activity (reviewed in reference 53) already under nutrient-replete conditions. Under starved conditions, ATP production could clearly be limiting (51, 52), leading to a need to produce extra ATP by other metabolic processes. Our data are consistent with this hypothesis, showing that when linear flow becomes limited by PSII in N^- cells, cyclic electron flow around PSI is stimulated by a factor of ~3 (Fig. 8D), indicating that the balance between NADPH and ATP generation is modified in these cells. Based on the evaluation of the rate of P_{700} rereduction after illumination (Fig. 8) (54) we can estimate that ~10 electrons are injected into PSI per second by a PSII-independent pathway. Therefore, we tend to exclude the possibility that the activity measured in the presence of DCMU reflects a nonphotochemical reduction of the intersystem electron carrier by a chlororespiratory pathway and consider that the DCMU-independent pathway represents a genuine cyclic electron flow process catalyzed by PSI photochemistry. Indeed, the observed rate is very close to the maximum estimate of cyclic electron flow under the same conditions in microalgae (54) and is larger than the one of chlororespiration in *Chlamydomonas* (55), i.e., an alga where this process is extremely efficient (56).

What is the physiological role of this energetic change? N limitation is well-known to induce the synthesis of triacylglycerols in several alga species, as also observed for *Nannochloropsis* (5, 19, 57). In *Chlamydomonas*, it has been demonstrated that at least part of this lipid accumulation comes from *de novo* synthesis (58), as we also observed here in the case of *Nannochloropsis*. In principle, the increased cyclic electron transport observed here could play a direct role in supplying energy for lipid biosynthesis (59). However, one must take into account the fact that lipid biosynthesis has a very high NADPH demand, and since this biosynthetic path occurs in the chloroplast, this NADPH should mostly be of photosynthetic origin. Therefore, enhancing cyclic flow, which provides only ATP, at the expense of linear flow, which generates both ATP and NADPH, should not produce any benefit in terms of energy availability for lipid biosynthesis. This apparently contradictory situation can be tackled by assuming that under N starvation conditions a nonnegligible part of the NADPH produced by the remaining LEF would be employed for fatty acid synthesis, while cyclic electron flow would be used to fuel ATP production for both carbon assimilation and other housekeeping purposes. Consistent with this possibility, activation of CEF under nutrient starvation conditions has often been observed in microalgae. In *Chlamydomonas*, phosphorus, sulfur, and nitrogen starvation induce a transition to state 2, a physiological condition where most

of the PSII light-harvesting proteins migrate toward PSI and the cyclic electron flow around PSI is largely enhanced (reviewed in reference 22). This would serve the purpose of both protecting PSII against inhibition and providing ATP for growth metabolic purposes.

In conclusion, our study of the molecular changes occurring in the photosynthetic electron flow chain of *Nannochloropsis* under conditions leading to oil accumulation reveals that, despite the large rearrangement of photosynthetic complexes during starvation, the remaining photosynthetic activity is sufficient to support triacylglycerol accumulation. It is worth underlining that the extent of galactolipid breakdown, which could be a critical process limiting photosynthesis following N starvation and subsequently provoke growth arrest, is kept to a level which does not impair chloroplast structure and functionality in *Nannochloropsis*. This suggests that the balance between triacylglycerol accumulation following the neosynthesis of fatty acids and diversion of preexisting membrane lipids is controlled, and this could be one of the parameters that might be used in the rational screening of microalgal strains for biofuel applications and, possibly, one of the factors that could be controlled in metabolic engineering strategies. Overall, this suggests a possible direction to engineer the cellular electron flow capacity to implement algal culture under oil-producing conditions.

ACKNOWLEDGMENTS

This work was supported by an FSE project from Regione Veneto (no. 2105/1/5/1739/2011) and ERC starting grant BIOLEAP (no. 309485) to T.M.; ANR grant (no. NT09_567009 Phytadapt) and the CNRS-JST strategic program on Marine Biology, Marine Biotechnology program, to G.F.; ANR-10-BLAN-01524-01 (ReGal) to E.M. and M.A.B; and ANR-12-BIME-0005 (DiaDomOil) from the CEA Nannocontrol program and the Labex GRAL to G.F. and E.M.

We also thank Stefania Basso (Università di Padova) for help in preliminary experiments and the Servizio di Microscopia Elettronica (Dipartimento di Biologia, Università di Padova) for help with the electron microscopy facilities.

REFERENCES

1. **Chisti Y, Yan JY.** 2011. Energy from algae: current status and future trends. Algal biofuels—a status report. Appl. Energy **88**:3277–3279.
2. **Malcata FX.** 2011. Microalgae and biofuels: a promising partnership? Trends Biotechnol. **29**:542–549.
3. **Balat M, Balat H.** 2008. A critical review of bio-diesel as a vehicular fuel. Energy Conversion Manage. **49**:2727–2741.
4. **Boussiba S, Vonshak A, Cohen Z, Avissar Y, Richmond A.** 1987. Lipid and biomass production by the halotolerant microalga Nannochloropsis-Salina. Biomass **12**:37–47.
5. **Rodolfi L, Chini ZG, Bassi N, Padovani G, Biondi N, Bonini G, Tredici MR.** 2009. Microalgae for oil: strain selection, induction of lipid synthesis and outdoor mass cultivation in a low-cost photobioreactor. Biotechnol. Bioeng. **102**:100–112.
6. **Bondioli P, Della BL, Rivolta G, Chini ZG, Bassi N, Rodolfi L, Casini D, Prussi M, Chiaramonti D, Tredici MR.** 2012. Oil production by the marine microalgae Nannochloropsis sp. F&M-M24 and Tetraselmis suecica F&M-M33. Bioresour. Technol. **114**:567–572.
7. **Breuer G, Lamers PP, Martens DE, Draaisma RB, Wijffels RH.** 2012. The impact of nitrogen starvation on the dynamics of triacylglycerol accumulation in nine microalgae strains. Bioresour. Technol. **124**:217–226.
8. **Gouveia L, Oliveira AC.** 2009. Microalgae as a raw material for biofuels production. J. Ind. Microbiol. Biotechnol. **36**:269–274.
9. **Recht L, Zarka A, Boussiba S.** 2012. Patterns of carbohydrate and fatty acid changes under nitrogen starvation in the microalgae Haematococcus pluvialis and Nannochloropsis sp. Appl. Microbiol. Biotechnol. **94**:1495–1503.
10. **Eltgroth ML, Watwood RL, Wolfe GV.** 2005. Production and cellular localization of neutral long-chain lipids in the haptophyte algae Isochrysis galbana and Emiliania huxleyi. J. Phycol. **41**:1000–1009.
11. **Adams C, Godfrey V, Wahlen B, Seefeldt L, Bugbee B.** 2012. Understanding precision nitrogen stress to optimize the growth and lipid content tradeoff in oleaginous green microalgae. Bioresour. Technol. **131C**: 188–194.
12. **Kolber Z, Zehr J, Falkowski P.** 1988. Effects of growth irradiance and nitrogen limitation on photosynthetic energy conversion in photosystem II. Plant Physiol. **88**:923–929.
13. **Berges JA, Charlebois DO, Mauzerall DC, Falkowski PG.** 1996. Differential effects of nitrogen limitation on photosynthetic efficiency of photosystems I and II in microalgae. Plant Physiol. **110**:689–696.
14. **Grossman A.** 2000. Acclimation of Chlamydomonas reinhardtii to its nutrient environment. Protist **151**:201–224.
15. **Miller R, Wu G, Deshpande RR, Vieler A, Gartner K, Li X, Moellering ER, Zauner S, Cornish AJ, Liu B, Bullard B, Sears BB, Kuo MH, Hegg EL, Shachar-Hill Y, Shiu SH, Benning C.** 2010. Changes in transcript abundance in Chlamydomonas reinhardtii following nitrogen deprivation predict diversion of metabolism. Plant Physiol. **154**:1737–1752.
16. **Merchant SS, Helmann JD.** 2012. Elemental economy: microbial strategies for optimizing growth in the face of nutrient limitation. Adv. Microb. Physiol. **60**:91–210.
17. **Greene RM, Geider RJ, Falkowski PG.** 1991. Effect of iron limitation on photosynthesis in a marine diatom. Limnol. Oceanogr. **36**:1772–1782.
18. **Kilian O, Benemann CS, Niyogi KK, Vick B.** 2011. High-efficiency homologous recombination in the oil-producing alga Nannochloropsis sp. Proc. Natl. Acad. Sci. U. S. A. **108**:21265–21269.
19. **Radakovits R, Jinkerson RE, Fuerstenberg SI, Tae H, Settlage RE, Boore JL, Posewitz MC.** 2012. Draft genome sequence and genetic transformation of the oleaginous alga Nannochloropis gaditana. Nat. Commun. **3**:686. doi:10.1038/ncomms1688.
20. **Lubian LM, Montero O, Moreno-Garrido I, Huertas IE, Sobrino C, Gonzalez-del Valle M, Pares G.** 2000. Nannochloropsis (Eustigmatophyceae) as source of commercially valuable pigments. J. Appl. Phycol. **12**: 249–255.
21. **Brown JS.** 1987. Functional organization of chlorophyll a and carotenoids in the alga, Nannochloropsis salina. Plant Physiol. **83**:434–437.
22. **Eberhard S, Finazzi G, Wollman FA.** 2008. The dynamics of photosynthesis. Annu. Rev. Genet. **42**:463–515.
23. **Joyard J, Ferro M, Masselon C, Seigneuri-Berny D, Salvi D, Garin J, Rolland N.** 2010. Chloroplast proteomics highlights the subcellular compartmentation of lipid metabolism. Prog. Lipid Res. **49**:128–158.
24. **Guillard RRL, Ryther JH.** 1962. Studies of marine planktonic diatoms. I. Cyclotella nana Hustedt and Detonula confervagea Cleve. Can. J. Microbiol. **8**:229–239.
25. **Folch J, Lees M, Sloane Stanley GH.** 1957. A simple method for the isolation and purification of total lipides from animal tissues. J. Biol. Chem. **226**:497–509.
26. **Bligh GE, Dyer WJ.** 1959. A rapid method of total lipid extraction and purification. Can. J. Biochem. Physiol. **37**:911–917.
27. **Li-Beisson Y, Shorrosh B, Beisson F, Andersson MX, Arondel V, Bates PD, Baud S, Bird D, Debono A, Durrett TP, Franke RB, Graham IA, Katayama K, Kelly AA, Larson T, Markham JE, Miquel M, Molina I, Nishida I, Rowland O, Samuels L, Schmid KM, Wada H, Welti R, Xu C, Zallot R, Ohlrogge J.** 2010. Acyl-lipid metabolism. Arabidopsis Book **8**:e0133. doi:10.1199/tab.0133.
28. **Moran R, Porath D.** 1980. Chlorophyll determination in intact tissues using N,N-dimethylformamide. Plant Physiol. **65**:478–479.
29. **Porra RJ, Thompson WA, Kriedemann PE.** 1989. Determination of accurate extinction coefficients and simultaneous equations for assaying chlorophylls a and b extracted with four different solvents: verification of the concentration of chlorophyll standards by atomic absorption spectroscopy. Biochim. Biophys. Acta **975**:384–394.
30. **Wellburn AR.** 1994. The spectral determination of chlorophyll-A and chlorophyll-B, as well as total carotenoids, using various solvents with spectrophotometers of different resolution. J. Plant Physiol. **144**:307–313.
31. **Farber A, Jahns P.** 1998. The xanthophyll cycle of higher plants: influence of antenna size and membrane organization. Biochim. Biophys. Acta **1363**:47–58.
32. **Laemmli UK.** 1970. Cleavage of structural proteins during the assembly of the head of bacteriophage T4. Nature **227**:680–685.
33. **Witt HT.** 1979. Energy conversion in the functional membrane of pho-

tosynthesis. Analysis by light pulse and electric pulse methods. The central role of the electric field. Biochim. Biophys. Acta **505**:355–427.
34. **Bailleul B, Cardol P, Breyton C, Finazzi G.** 2010. Electrochromism: a useful probe to study algal photosynthesis. Photosynth. Res. **106**:179–189.
35. **Finazzi G, Buschlen S, De Vitry C, Rappaport F, Joliot P, Wollman FA.** 1997. Function-directed mutagenesis of the cytochrome b6f complex in Chlamydomonas reinhardtii: involvement of the cd loop of cytochrome b6 in quinol binding to the Q(o) site. Biochemistry **36**:2867–2874.
36. **Demmig-Adams B, Adams WW, Barker DH, Logan BA, Bowling DR, Verhoeven AS.** 1996. Using chlorophyll fluorescence to assess the fraction of absorbed light allocated to thermal dissipation of excess excitation. Physiol. Plant. **98**:253–264.
37. **Joliot P, Joliot A.** 2006. Cyclic electron flow in C3 plants. Biochim. Biophys. Acta **1757**:362–368.
38. **Morosinotto T, Segalla A, Giacometti GM, Bassi R.** 2010. Purification of structurally intact grana from plants thylakoids membranes. J. Bioenerg. Biomembr. **42**:37–45.
39. **Boudiere L, Botte CY, Saidani N, Lajoie M, Marion J, Brehelin L, Yamaryo-Botte Y, Satiat-Jeunemaitre B, Breton C, Girard-Egrot A, Bastien O, Jouhet J, Falconet D, Block MA, Marechal E.** 2012. Galvestine-1, a novel chemical probe for the study of the glycerolipid homeostasis system in plant cells. Mol. Biosyst. **8**:2023–2035.
40. **Petrie JR, Vanhercke T, Shrestha P, El Tahchy A, White A, Zhou XR, Liu Q, Mansour MP, Nichols PD, Singh SP.** 2012. Recruiting a new substrate for triacylglycerol synthesis in plants: the monoacylglycerol acyltransferase pathway. PLoS One **7**:e35214. doi:10.1371/journal.pone.0035214.
41. **Niyogi KK, Björkman O, Grossman AR.** 1997. The roles of specific xanthophylls in photoprotection. Proc. Natl. Acad. Sci. U. S. A. **94**:14162–14167.
42. **Maxwell K, Johnson GN.** 2000. Chlorophyll fluorescence—a practical guide. J. Exp. Bot. **51**:659–668.
43. **Butler WL, Kitajima M.** 1975. Fluorescence quenching in photosystem II of chloroplasts. Biochim. Biophys. Acta **376**:116–125.
44. **Butler WL, Tredwell CJ, Malkin R, Barber J.** 1979. The relationship between the lifetime and yield of the 735nm fluorescence of chloroplasts at low temperatures. Biochim. Biophys. Acta **545**:309–315.
45. **Jones RW, Whitmarsh J.** 1988. Inhibition of electro N^- transfer and the electrogenic reaction in the cytochrome B/F complex by 2-normal-nonyl-4-hydroxyquinoline N^- oxide (Nqno) and 2,5-dibromo-3-methyl-6-isopropyl-P-benzoquinone (Dbmib). Biochim. Biophys. Acta **933**:258–268.
46. **Sforza E, Cipriani R, Morosinotto T, Bertucco A, Giacometti GM.** 2012. Excess CO_2 supply inhibits mixotrophic growth of Chlorella protothecoides and Nannochloropsis salina. Bioresour. Technol. **104**:523–529.
47. **Li X, Moellering ER, Liu B, Johnny C, Fedewa M, Sears BB, Kuo MH, Benning C.** 2012. A galactoglycerolipid lipase is required for triacylglycerol accumulation and survival following nitrogen deprivation in Chlamydomonas reinhardtii. Plant Cell **24**:4670–4686.
48. **Li Z, Wakao S, Fischer BB, Niyogi KK.** 2009. Sensing and responding to excess light. Annu. Rev. Plant Biol. **60**:239–260.
49. **Nixon PJ, Michoux F, Yu J, Boehm M, Komenda J.** 2010. Recent advances in understanding the assembly and repair of photosystem II. Ann. Bot. **106**:1–16.
50. **Bulte L, Wollman FA.** 1992. Evidence for a selective destabilization of an integral membrane protein, the cytochrome b6/f complex, during gametogenesis in Chlamydomonas reinhardtii. Eur. J. Biochem. **204**:327–336.
51. **Allen J.** 2002. Photosynthesis of ATP-electrons, proton pumps, rotors, and poise. Cell **110**:273–276.
52. **Behrenfeld MJ, Halsey KH, Milligan AJ.** 2008. Evolved physiological responses of phytoplankton to their integrated growth environment. Philos. Trans. R. Soc. Lond. B Biol. Sci. **363**:2687–2703.
53. **Cardol P, Forti G, Finazzi G.** 2011. Regulation of electron transport in microalgae. Biochim. Biophys. Acta **1807**:912–918.
54. **Alric J, Lavergne J, Rappaport F.** 2010. Redox and ATP control of photosynthetic cyclic electron flow in Chlamydomonas reinhardtii (I) aerobic conditions. Biochim. Biophys. Acta **1797**:44–51.
55. **Houille-Vernes L, Rappaport F, Wollman FA, Alric J, Johnson X.** 2011. Plastid terminal oxidase 2 (PTOX2) is the major oxidase involved in chlororespiration in Chlamydomonas. Proc. Natl. Acad. Sci. U. S. A. **108**:20820–20825.
56. **Jans F, Mignolet E, Houyoux PA, Cardol P, Ghysels B, Cuine S, Cournac L, Peltier G, Remacle C, Franck F.** 2008. A type II NAD(P)H dehydrogenase mediates light-independent plastoquinone reduction in the chloroplast of Chlamydomonas. Proc. Natl. Acad. Sci. U. S. A. **105**:20546–20551.
57. **Simionato D, Sforza E, Corteggiani CE, Bertucco A, Giacometti GM, Morosinotto T.** 2011. Acclimation of Nannochloropsis gaditana to different illumination regimes: effects on lipids accumulation. Bioresour. Technol. **102**:6026–6032.
58. **Fan J, Andre C, Xu C.** 2011. A chloroplast pathway for the de novo biosynthesis of triacylglycerol in Chlamydomonas reinhardtii. FEBS Lett. **585**:1985–1991.
59. **Wilhelm C, Jakob T.** 2011. From photons to biomass and biofuels: evaluation of different strategies for the improvement of algal biotechnology based on comparative energy balances. Appl. Microbiol. Biotechnol. **92**:909–919.